FT-IR Microscopic Analysis of Changing Cellulose Crystalline Structure during Wood Cell Wall Formation

Yutaka Kataoka and Tetsuo Kondo*

Forestry and Forest Products Research Institute (FFPRI), P.O. Box 16, Tsukuba Norin, 305 Japan

Received May 30, 1997; Revised Manuscript Received October 13, 1997

ABSTRACT: A Fourier transform infrared (FT-IR) spectrometer equipped with a microscopic accessory was used to monitor the cellulose crystalline structure at each developmental stage of coniferous tracheid cell wall formation. The spectra showed that the cellulose in the primary cell wall was rich in the metastable I_α crystalline form and interestingly had a higher crystallinity than the secondary wall cellulose composed mainly of the stable I_β crystalline phase. These results indicate the presence of an in vivo physical force at the cell surface which may stress the primary wall cellulose during the crystallization. Moreover, the primary wall cellulose was oriented parallel to the enlarging direction of growing cells. Thus, we consider that the cellular growing stress generated between the plasma membrane and the primary wall may elongate just-biosynthesized β-glucan chains and cause them to crystallize with a higher crystallinity of the metastable I_α phase, as is the case for crystallization occurring during the drawing of polymer gels.

Introduction

Since the discovery of the dimorphism of native cellulose by Attala and VanderHart,[1] two mechanisms of in vivo crystallization for cellulose I_α and I_β allomorphs have been extensively studied.[2−6] These studies suggested that the occurrence of the metastble I_α phase may be attributed to some stress or strain to the crystallization of cellulose. To date, however, the whole system for the alternative crystallization of either I_α or I_β has not been clarified.

In a previous paper,[2] we examined cellulose crystalline structure changing during cell wall formation of coniferous tracheids with a combination of FT-IR spectroscopy and a microscopic technique. The results provided in vivo evidence that the major cellulose crystalline form changes from the primary to the secondary walls. First, the metastable I_α phase is mainly formed in the primary wall as the cells undergo enlarging growth and then, after ceasing of the cellular enlargement, the stable I_β phase becomes dominant in the secondary wall cellulose. Thus, we proposed that there may be some type of in vivo stress exerted at the cell surface with cellular enlarging growth and that it causes the nascent primary wall cellulose to crystallize in the metastable triclinic I_α phase, whereas in the secondary wall lack of stress results preferably in the stable monoclinic I_β phase crystallization.

In this paper, to confirm the effects of in vivo stress on the crystallization of cellulose, we attempted to monitor the cellulose crystalline structure changing not only in crystalline form but also in crystallinity as well as molecular orientation during wood cell wall formation. For this purpose, we employed a FT-IR spectrometer equipped with a microscopic accessory. Without damaging cellulose, this method enabled us to focus on each developmental stage of cell wall formation that appeared on a small section sample of developing wood xylem. In vivo evidences we thus obtained provided an important insight for the mechanism of cellulose I_α and I_β crystallization.

Experimental Section

Materials. (i) Standard Cellulose Samples. *Valonia ventricosa* cellulose and *Halocynthia rorezi* cellulose were purified by 2.5 N hydrochloric acid treatment and then washed thoroughly with distilled water and preserved in ethanol. *V. ventricosa* and *H. rorezi* were used as standard cellulose samples rich in the I_α crystalline phase and pure I_β, respectively. Purified cotton cellulose powder purchased from Toyo Roshi Co. Ltd. was also used as a standard sample of I_β-rich cellulose after it was subjected to 5% KOH treatment and washing with distilled water.

(ii) Wood Sample Preparation. *Chamaecyparis obtusa* (Japanese hinoki cypress) grown in Japan was felled at 28 years when it was forming ordinary spring wood xylem. As shown in Figure 1, sample blocks including differentiating wood xylem were cut from their trunks at breast height and immediately fixed with 3% glutaraldehyde at pH 6.8 in a phosphate buffer. Then, 30-μm-thick sections in the radial direction to wood annual rings were cut from the sample blocks with a prefrozen microtome. In these sections, developing axial tracheid cells as well as their cell walls lined up along a radial row in order of maturity, starting from the cambial zone to the mature xylem. Four stages (P, P + S_1, P + S_1 + S_2, P + S_1 + S_2 + S_3) of cell wall development appeared on the radial face of the sections. In general, first the primary wall (P) is formed during cellular radial enlarging growth (RE), and then the outer (S_1), middle (S_2), and inner (S_3) layers of the secondary wall are successively deposited onto the inner surface of the preformed wall layers.[7] The wood sections were then disencrusted thoroughly with a multiple combination of two purification methods for the primary wall[8] and the wood secondary wall[9] to completely remove pectin, polysaccharides, lignin, and other noncellulosic substances: The sections washed with distilled water were immersed overnight in chloroform−ethanol [1:1 (v/v)] and then transferred into acetone. After acetone was replaced by distilled water, the samples were subjected to water extraction at 90 °C for 6 h and 0.5% ammonium oxalate treatments at 70 °C for another 6 h. They were then extracted twice with 0.3% dodecyl sulfate for 12 h and with an aqueous solution of 50% urea for another

* To whom correspondence should be addressed.
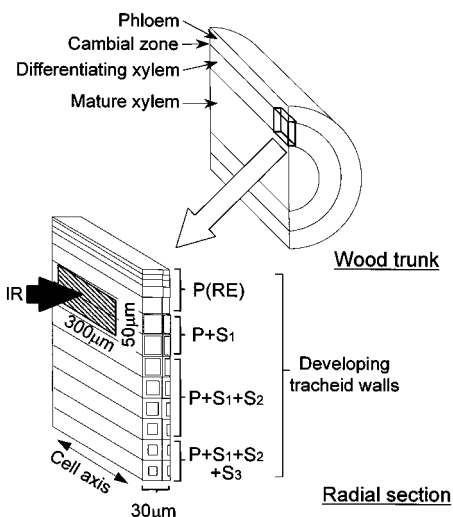
Figure 1. Method for obtaining IR spectra from each stage of tracheid cell wall formation: P, the primary wall just-formed during radial enlargement (RE) of tracheid cells; S_1, S_2 and S_3, deposition of the outer, middle, and inner layers of the secondary wall onto the preformed wall.

Figure 2. Decreases of the IR bands due to noncellulosic contaminants during the sample purification process (from the top to the bottom) in the spectra for the primary wall cellulose of Japanese cypress. The bands around 1600 cm^{-1} (marked by black arrows) indicate the noncellulosic contaminants, whereas white arrows indicate the typical position for cellulose I_α.

12 h at room temperature. Then, the wood sections were subjected to bleaching at 80 °C for 4 h in a 0.3% $NaClO_2$ aqueous solution buffered with acetic acid at pH 4.9 and then to overnight immersion in 5% KOH at room temperature. The sections were finally washed thoroughly again in distilled water and freeze-dried with *tert*-butyl alcohol before FT-IR analysis. All treatments described above were achieved by gentle shaking of samples in each solution.

Infrared Spectroscopy with a Microscopic Attachment. A FT-IR spectrometer (Nicolet Magna 550) was used. We obtained all spectra on small areas (300 × 50 μm^2) using a microscopic attachment (Nicolet Nic plan) which was focused on the radial face of the sections as shown in Figure 1. This method enabled us to analyze cellulose from four developmental stages (P, P + S_1, P + S_1 + S_2, P + S_1 + S_2 + S_3) of tracheid cell wall formation.[2] To distinguish between cellulose I_α and I_β crystalline forms, the characteristic IR bands, 750 cm^{-1} for I_α and 710 cm^{-1} for I_β,[5] were analyzed. The spectra were the average of 64 scans recorded at a resolution of 4 cm^{-1} in the range from 4000 to 600 cm^{-1} with a MCT detector, and they were normalized on the peak at 1060 cm^{-1} attributed to a CO stretching mode except for the polarized ones. Only spectra in the absorbance range from 0.30 to 0.022 (50−95% in a transmittance mode) were employed. It was confirmed for spectra from *V. ventricosa* and cotton cellulose that the thickness or shape of the samples did not affect the intensity ratios between the IR absorptions characteristic for the two crystalline forms (750 and 710 cm^{-1}) and the IR crystallinity index (1427 and 895 cm^{-1}).

IR Crystallinity Index. The IR crystallinity index of cellulose[10] was evaluated as the intensity ratio between IR absorptions at 1427 and 895 cm^{-1} which are assigned to CH_2 bending mode[11] and deformation of anomeric CH,[12] respectively. To obtain the correlation between IR and X-ray[13] crystallinity indices, we compared both values for purified *V. ventricosa* (rich in cellulose I_α) and cotton (rich in I_β) cellulose samples with a variety of crystallinities prepared by rod-milling.[14,15]

Molecular Orientation of Cellulose. To compare the molecular orientation of cellulose, FT-IR spectra were obtained with a polarizer for the primary (P) and the mature (P + S_1 + S_2 + S_3) walls in the sample from the Japanese cypress. We focused on the band at 1160 cm^{-1} due to COC stretching mode parallel to molecular chains.[11] Changes of this band intensity with a rotation of the polarizer from the tracheid cell axis (0°) to its perpendicular direction (90°) were examined by every 10°. The changes in the polarized spectra indicated the direction and degree of cellulose molecular orientation.

Results and Discussion

Crystalline Form Changing from I_α to I_β. As reported in a previous paper,[2] FT-IR spectra obtained from Japanese cypress and cedar showed that the cellulose in the primary wall was rich in the I_α phase, whereas after the start of the secondary wall deposition the I_β phase became dominant. This change indicates the presence of a particular driving force that may stress the crystallization of the primary wall cellulose. Such in vivo stress could have other effects on the crystalline structure. In this study using Japanese cypress, we tried to monitor changes in crystallinity and molecular orientation of cellulose which may be accompanied with the change of the crystalline form during cell wall formation.

Change of the Crystallinity during Cell Wall Formation. By the end of the purification for the wood section, IR absorptions due to noncellulosic polysaccharides, lignin, and other contaminants were greatly decreased as shown from the top to the bottom spectra in Figure 2. In particular, the absorptions at 1700−1500 cm^{-1} diminished to reach a negligible extent compared to those for purified standard cellulose from *V. ventricosa* and *H. rorezi* mentioned earlier. Finally, in the spectra of purified wood cellulose samples the absorption band due to I_α at 750 cm^{-1} appeared for the primary wall (Figure 2). This band became weak after the deposition of the secondary walls to show that the major cellulose component changed from I_α to I_β as reported in our previous paper.[2]

Figure 3 shows how the IR crystallinity index of cellulose changed during the cell wall formation of Japanese cypress tracheid. As growing cells were forming their primary walls, the index slightly increased to ca. 2.8. The corresponding X-ray crystallinity index for this value was about 70% on the basis of the correlation curve as shown in Figure 4. However, once the secondary wall started to deposit, the IR crystallinity index tended to decrease until it reached 2.1 (about 60% in X-ray index) in the midst of the secondary wall formation. Thus, the primary wall cellulose proved to be of higher crystallinity than the secondary wall cellulose. Since cellulose crystalline forms are different between the primary and the secondary walls as de-
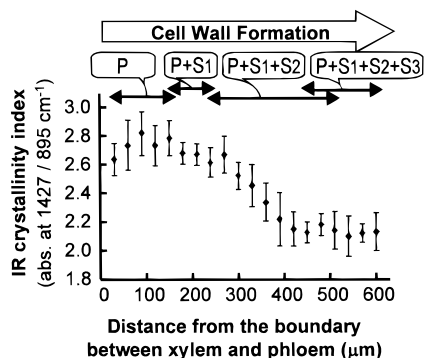
Figure 3. Change of the IR crystallinity index of cellulose during cell wall formation of Japanese cypress tracheid. The results are averages of six areas analyzed at every 30 μm from the boundary between xylem and phloem (the earliest stage of primary wall formation) to mature xylem.
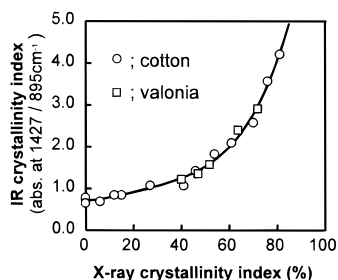
Figure 4. Correlation between X-ray and IR crystallinity indices of cellulose for cotton (rich in I_β) and *V. ventricosa* (rich in I_α) with different degrees of crystallinity prepared by rod-milling.

scribed above, it is not generally effective to compare two different crystalline types in the same crystallinity index. Nevertheless, the trace in Figure 4 displays a good correlation between IR and X-ray crystallinity indices regardless of the difference of the crystalline form, I_α or I_β, suggesting that our results for IR crystallinity were not dependent on the difference of crystalline form. The change of crystallinity supports the hypothesis that β-glucan chains in the nascent primary wall cellulose may be stressed along molecular chains during crystallization. The stress accompanied with cellular growth may cause the glucan chains in the primary wall cellulose to crystallize mainly in the metastable I_α form with a higher crystallinity. Such a drawing effect causing a metastable triclinic form can also be found for the crystallization of drawn polyethylene gel.[16] In addition, it is interesting that the crystallinity index in Figure 3 seems to start decreasing with the deposition of the S_2 layer. It might be related to a tracheid enlarging system which has recently been suggested to continue through the primary wall formation to the earliest stage of the secondary wall deposition.[17] Thus, we consider that at the earliest stage (S_1) of the secondary wall formation the enlarging stress remains possibly to cause higher crystallinity although it may not be enough to induce I_α.

The above suggestion is really contrary to that due to previous X-ray and electron diffraction studies which reported that the crystallinity of primary wall cellulose may be lower than that for secondary wall cellulose[18] partly because the cellulose is disorganized[8] or totally amorphous[19] in the primary wall. Of course, this discrepancy may be dependent on measurements for different sorts of plant species. In addition, these studies might underestimate the crystallinity for pri-
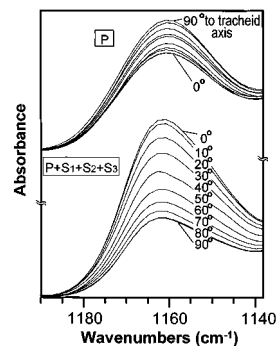
Figure 5. Changes in FT-IR spectra with a rotation of IR polarizer from parallel (0°) to perpendicular (90°) to the tracheid cell axis at 1160 cm^{-1} due to the C−O−C stretching mode for the primary (P) and the mature (P + S_1 + S_2 + S_3) walls of Japanese cypress tracheid.

mary wall cellulose. For example, cellulose microfibrils are densely arranged in the secondary wall, while the orientation in the primary wall is coarser.[20] Therefore, it is difficult to completely avoid the morphological effects due to packing density and molecular orientation of cellulose on the X-ray crystallinity index.[13,21] Even sample preparation processes, such as drying and trimming, may result in an underestimation of the primary wall cellulose because its orientation in the thin primary wall can be distorted more easily than that in the thick and dense secondary wall through the same treatment. In fact, for the dried tracheid primary wall, it was found that cellulose microfibrils were poorly oriented[20] although our AFM (atomic force microscopic) data indicate that before drying they may originally be oriented more parallel.[22] Thus, the above synchronous results on the change of both crystalline form and the crystallinity of cellulose may reasonably reflect in situ change during cell wall formation.

Molecular Orientation of Cellulose. The above results suggest that β-glucan chains in the nascent primary wall cellulose may be stressed along molecular chains during crystallization. To confirm the drawing effect, we examined the direction and the degree of molecular orientation during cell wall formation. The IR band intensity at 1160 cm^{-1} (COC stretching mode for glucose rings) was monitored by rotating a polarizer from the tracheid cell axis (0°) to its perpendicular direction (90°). Results are shown in Figure 5. The strongest and weakest band intensities showed that the main orientation of the primary wall cellulose (P) was found to be perpendicular (90°) to the cell axis, whereas that for the mature wall (P + S_1 + S_2 + S_3) was parallel to it (0°). The orientation of the primary wall cellulose coincided with the direction of cellular enlarging growth, corresponding to the previous microscopic observations of cellulose microfibrils.[20] This suggests that the primary wall cellulose may be oriented during crystallization and subsequent formation of microfibrils by the drawing effect exerted during cellular enlargement. On the other hand, the degree of orientation was difficult to examine especially for the primary wall. The traces for the primary wall cellulose in Figure 5 indicate less orientation of the molecules than that in the secondary wall. However, the original orientation of the primary wall cellulose should be more or less reduced especially during the sample drying process.[22] Consequently, the discussion about the degree of orientation requires further investigation from samples free of drying effects.
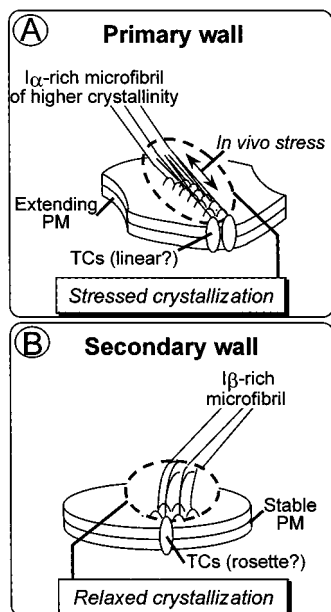
Figure 6. Schematic representations of stressed (A) and relaxed (B) crystallization forms for I_α-rich primary (P) wall cellulose and I_β-rich secondary (S) wall cellulose, respectively. The areas encircled by dotted lines indicate the manner of crystallization occurring between the plasma membrane (PM) and β-glucan chains in the cell wall. The stress to the nascent molecules may also determine the two types of arrangement of cellulose-synthesizing terminal enzyme complexes (TCs).

In the present study, to confirm in vivo stress for the crystallization of cellulose, we have examined coniferous tracheid cellulose changing in crystalline form, crystallinity, and orientation during cell wall formation. These changes synchronized with the cellular and cell wall development, indicating the presence of drawing effects for the crystallization of the primary wall cellulose. First, during cellular enlarging growth, the primary wall cellulose was of higher crystallinity and rich in the triclinic metastable I_α crystalline phase, which is considered as a strain-induced form.[4-6] Then, after ceasing of cellular enlargement, the monoclinic stable I_β, which is believed to be strain-free,[4-6] became dominant in the secondary wall cellulose with a reduction of crystallinity. Moreover, the main chain orientation of the primary wall cellulose was parallel to the cellular enlarging direction. The results lead to the suggestion that nascent primary wall cellulose may be driven by the drawing stress exerted with cellular enlarging growth. This force along molecular chains can cause β-glucan chains in the nascent cellulose to crystallize in the I_α phase with a higher crystallinity, making the molecules orient in the enlarging direction. There might be other effects involved in the crystallization, such as the affinity of other polysaccharides for cellulose[6,23] and the arrangement of the TCs (cellulose-synthesizing terminal enzyme complexes).[5,24] However, the drawing of the glucan chains in the nascent cellulose differs from other effects because it can simultaneously cause the alterations of crystalline form, crystallinity, and molecular orientation, as is the case for the crystallization of a metastable triclinic crystalline form found in drawn polyethylene gels.[16]

Outlook

A Model of Crystallization for I_α and I_β in Wood Cell Walls. As a concluding remark, we propose the

following model of crystallization for I_α and I_β which may occur at the cell surface of tracheid: As illustrated in Figure 6, just-biosynthesized β-glucan chains can easily be stressed along the molecular chains because both ends of the molecule are bound to the TCs on the plasma membrane (PM) and to the cell wall, respectively. In particular, during the primary wall formation of enlarging tracheid cells, there should be more stresses between extending PM and the stretched wall. Thus, the glucan chains in the nascent cellulose in a mesomorphic state should be strained along the molecular chains to preferably crystallize in the strain-induced I_α phase with a higher crystallinity (A in Figure 6). On the other hand, after ceasing of the cellular enlargement, the secondary wall cellulose is formed in a relatively relaxed environment which should favor the strain-free I_β phase crystallization (B in Figure 6).

There is a hypothesis that the appearance of two cellulose allomorphs can be correlated with the two typical arrangements of the TCs.[5,24] To date their arrangement has not been observed for coniferous tracheid. If they exist, however, considering the stress against crystallization mentioned above, we want to notify that the stress may physically determine not only the cellulose crystalline structure but also the TCs arrangement by drawing nascent molecules bound to both crystalline and TCs phases.

References and Notes

(1) Atalla, R. H.; VanderHart, D. L. *Science* **1984**, *223*, 283–285.
(2) Kataoka, Y.; Kondo, T. *Macromolecules* **1996**, *29*, 6356–6358.
(3) Horii, F.; Yamamoto, H.; Kitamaru, R.; Tanahashi, M.; Higuchi, T. *Macromolecules* **1987**, *20*, 2946–2949.
(4) Sugiyama, J.; Okano, T.; Yamamoto, H.; Horii, F. *Macromolecules* **1990**, *23*, 3196–3198.
(5) Sugiyama, J.; Persson, J.; Chanzy, H. *Macromolecules* **1991**, *24*, 2461–2466.
(6) Yamamoto, H.; Horii, F. *Cellulose* **1994**, *1*, 57–66.
(7) Kataoka, Y.; Saiki, H.; Fujita, M. *Mokuzai Gakkaishi* **1992**, *38*, 327–335.
(8) Chanzy, H.; Imada, K.; Vuong, R.; Barnoud, F. *Protoplasma* **1979**, *100*, 303–316.
(9) Wada, M.; Sugiyama, J.; Okano, T. *Mokuzai Gakkaishi* **1994**, *40*, 50–56.
(10) Nelson, M. L.; O'Connor, R. T. *J. Appl. Polym. Sci.* **1964**, *8*, 1325–1341.
(11) Liang, C. Y.; Marchessault, R. H. *J. Polym. Sci.* **1959**, *37*, 385–395.
(12) Blackwell, J.; Vasko, P. D.; Koenig, J. L. *J. Appl. Phys.* **1970**, *41*, 4375–4379.
(13) Jayme, G.; Knolle, H. *Papier (Darmstadt)* **1964**, *18*, 249–255.
(14) Hess, K.; Kiessig, H.; Gundermann, J. *Z. Phys. Chem. (Leipzig)* **1941**, *B49*, 64.
(15) Hermans, P. H.; Weidinger, A. *J. Am. Chem. Soc.* **1946**, *68*, 2547.
(16) Chanzy, H.; Smith, P.; Revol, J.-F.; Manley, R. St. J. *Polym. Commun.* **1987**, *28*, 133–136.
(17) Abe, H.; Funada, R.; Ohtani, J.; Fukazawa, K. *Trees* **1997**, *11*, 328–332.
(18) (a) Hanna, R. B.; Côte, W. A., Jr. *Cytobiologie* **1974**, *10*, 102–116 (for wood cellulose). (b) Hu, X.-P.; Hsieh, Y.-L. *J. Polym. Sci., Part B* **1996**, *34*, 1451–1459 (for cotton cellulose).
(19) Nowak-Ossorio, M.; Gruber, E.; Schurz, J. *Protoplasma* **1976**, *88*, 255 (for cotton cellulose).
(20) (a) Wardrop, A. B. In *The Formation of Wood in Forest Trees*; Zimmermann, M. H., Ed.; Academic Press: New York, 1964;

pp 87−134. (b) Abe, H.; Funada, R.; Ohtani, J.; Fukazawa, K. *Ann. Bot. (London)* **1995**, *75*, 305−310.

(21) Watanabe, S.; Akahori, T.; Matsubara, H. *Bull., Fac. Eng., Hokkaido Univ.* **1967**, *43*, 111−129.

(22) Kataoka, Y.; Kondo, T., unpublished data.

(23) (a) Attala, R. H.; Hackney, J. M.; Uhlin, I.; Thompson, N. S. *Int. J. Biol. Macromol.* **1993**, *15*, 109−112. (b) Vian, B.; Reis, D.; Darzens, D.; Roland, J. C. *Protoplasma* **1994**, *180*, 70−81.

(24) (a) Attala, R. H.; VanderHart, D. L. In *Cellulose and Wood− Chemistry and Technology*; Schuerch, C., Ed.; Wiley-Interscience: New York, 1989; pp 169−188. (b) Wada, M.; Sugiyama, J.; Okano, T. *Mokuzai Gakkaishi* **1995**, *41*, 186−192.